

DFT and TB-mBJLDA studies of structural, electronic and optical properties of $\text{Hg}_{1-x}\text{Cd}_x\text{Te}$ and $\text{Hg}_{1-x}\text{Zn}_x\text{Te}$

N. Aouail^a, M. Noureddine Belkaid^b, A. Oukebdane^c, and M. Hocine Tedjini^d

*Laboratory for Analysis and Application of Radiation, Department of Physics, Faculty of Physics,
University of Sciences and Technology of Oran Mohamed Boudiaf,
BP1505 ElMenaouer, Oran31000, Algeria.*

*e-mail: nouria.aouail@gmail.com; mnbekaid@gmail.com;
oazizdz@yahoo.com; tedjini.mohammedhocine@gmail.com

Received 11 January 2021; accepted 16 March 2021

In this paper, the fundamental semiconductor properties of $\text{Hg}_{1-x}\text{Cd}_x\text{Te}$ and $\text{Hg}_{1-x}\text{Zn}_x\text{Te}$ are investigated by ab initio calculations based on the FPLAPW method. Structural properties have been calculated using LDA and GGA approximations. The electronic properties are studied using the LDA and GGA approximations and the potential TB-mBJLDA coupled with the lattice parameters aLDA and aGGA. The optical properties are determined from the optimal gap energies based on the TB-mBJLDA potential. Lattice parameters aLDA obtained by the LDA calculations predict values that are in good agreement with the experimental results and are better than those results obtained by the GGA calculations. The use of TB-mBJLDA potential coupled with the lattice parameter aGGA gives gap energy values in good agreement with the experimental results for all alloys except $\text{Hg}_{1-x}\text{Zn}_x\text{Te}$ ($x = 0.5, 0.75$) where the (TB-mBJLDA+aLDA) is more suitable. Optical constants are calculated from the dielectric function in the energy range (0–30 eV). The spectrum of real and imaginary parts of the dielectric function, the energy loss function, the refractive index, the extinction coefficient, the absorption coefficient, and the reflectivity show that optical properties of $\text{Hg}_{1-x}\text{Cd}_x\text{Te}$ are comparable to those of $\text{Hg}_{1-x}\text{Zn}_x\text{Te}$. Our results are found to be in reasonable agreement with existing data reported in the literature.

Keywords: Ab initio; FPLAPW; TB-mBJLDA; gap energy; optical properties.

PACS: 42.70.-a; 31.15.Ar; 61.82.Fk; 71.15.Mb; 71.20.-b; 73.20.At

DOI: <https://doi.org/10.31349/RevMexFis.67.061003>

1. Introduction

Mercury-cadmium telluride $\text{Hg}_{1-x}\text{Cd}_x\text{Te}$ and Mercury-Zinc Telluride $\text{Hg}_{1-x}\text{Zn}_x\text{Te}$ are two competitive materials used in infrared radiation detection [1,2]. They have important applications in medicine and biology (laser IR, infrared camera) [3], in the industry (control of food products, rubber industry...) [4,5], and security (surveillance in military fields) [6]. They are also used as Solar cells and photo-conductors [2-7-8]. These are pseudo-binary semiconductors in the (II-VI) groups with small gaps and the same structural properties [9,10]. The gap energies of the $\text{Hg}_{1-x}\text{Cd}_x\text{Te}$ alloys are between -0.3 eV (HgTe) and 1.6 eV (CdTe) and fall within the infrared radiation energy range (IR) [$E \leq 1.65$ eV]. However, the $\text{Hg}_{1-x}\text{Zn}_x\text{Te}$ possesses gap energies from -0.3 eV (HgTe) to 2.38 eV (ZnTe) and mechanical hardness that is greater than those of the $\text{Hg}_{1-x}\text{Cd}_x\text{Te}$. These alloys are found to have the same nature of gaps [11,12].

Recently, M. Debbarma *et al.*, [13] investigated the elastic and thermal properties of zinc Blende $\text{Hg}_{1-x}\text{Cd}_x\text{Te}$ ternary alloys using the FP-LAPW method. F. Kadari *et al.*, [14] used WIEN2K code to study the structural properties of $\text{Hg}_{1-x}\text{Cd}_x\text{Te}$ and $\text{Hg}_{1-x}\text{Zn}_x\text{Te}$ alloys and the electronic properties of $\text{Hg}_{1-x}\text{Cd}_x\text{Te}$ and $\text{Hg}_{1-x}\text{Zn}_x\text{Te}$ alloys for $X = 0.5$ within the PBE-GGA and WC-GGA approximations in the zinc blende structure. The TB-mBJGGA potential combined with the PBE-GGA approximation was again

used to study the electronic properties of the same materials. The results obtained are in agreement with experimental data. A. Laref *et al.*, [15] studied the electronic structure, and optical characteristics of ZnHgTe alloys at concentrations $x = 0.25, 0.50, 0.75$ by using the mBJ-GGA approach. S. Al-Rajoub and B. Hamad [16] have studied the structural, electronic, and optical properties of the ternary alloy $\text{Hg}_{1-x}\text{Cd}_x\text{Te}$ ($X = 0.0, 0.25, 0.5$ and 0.75), using WIEN2K code. In the same study, calculations of the structural properties are carried out with the LDA and GGA approximations for $X = 0.0, 0.25$, and 0.75 in the zinc blende structure and the tetragonal structure for $X = 0.5$. However, the electronic properties are determined with different approximations, namely: LDA, GGA, (LDA/GGA) + U, and (LDA / GGA) +mBJ. The mBJ+GGA approach gives better results for the electronic properties, except in the case of HgTe, where the GGA+U is better. The dielectric function was calculated using data obtained from the approximations giving the best gap values. B.V. Robouch *et al* [17] presented experimental results of the optical properties (dielectric function and reflectivity) of $\text{Hg}_{1-x}\text{Cd}_x\text{Te}$ and $\text{Hg}_{1-x}\text{Zn}_x\text{Te}$ for different concentrations. To our knowledge, there are no results published on the optical properties of $\text{Hg}_{1-x}\text{Zn}_x\text{Te}$ alloys for $X = 0.25, 0.5$, and 0.75 except Laref *et al.*, [15]. Moreover, there are no published results on the absorption spectrum of $\text{Hg}_{1-x}\text{Cd}_x\text{Te}$, the refractive, and the reflection indexes of $\text{Hg}_{1-x}\text{Cd}_x\text{Te}$ ($X=0.25, 0.75$). Our contribution to

the research topic is the use of two theoretical approaches, namely, the DFT and TB-mBJLDA for a detailed investigation of electronic and optical properties. To show the importance of the lattice parameter values in the computation of gap energy, the lattice parameter optimized either by LDA or GGA approximation has been used as an input parameter of the ‘TB-mBJLDA’ approach. As for the optical properties, a more comprehensive study and a detailed analysis of the optical coefficients, namely, the absorption spectrum, the refractive, and reflectivity index has been carried out an aspect that has found little interest in the published theoretical results in the literature.

The DFT is known for its underestimation of the gap energy [18], which has a direct impact on the computation of physical properties that are functions of gap energy, namely the linear optical properties [14]. The option of using the DFT combined with the TB-mBJLDA potential [19] is considered, knowing that small variations of the lattice parameter values may generate important variations in the gap energy [20]. In this work, the DFT (LDA and GGA) is used for the optimization of the lattice parameter of $Hg_{1-x}Cd_xTe$ and $Hg_{1-x}Zn_xTe$ for $X = 0.0, 0.25, 0.5, 0.75$, and 1.0 . A comparative study of the electronic properties of these materials is carried out. It consists in performing a series of ab-initio calculations (LDA and GGA) with and without the TB-mBJLDA potential. Previous work using the TB-mBJLDA [21] has proved that the approach is successful for determining electronic and optical properties. Results from the first principle calculations are used to compute optical properties of $Hg_{1-x}Cd_xTe$ and $Hg_{1-x}Zn_xTe$ alloys in the zinc-blende structure at concentrations X in the range (0,1). The determination of the dielectric function will use data based on the approach giving the best gap energy. Our objective is to complete previous theoretical works regarding the structural, electronic, and mainly optical properties of $Hg_{1-x}Cd_xTe$ and $Hg_{1-x}Zn_xTe$ alloys for different values of X . In the following, the methodology is exposed, followed by an analysis of the obtained results and a conclusion.

2. Computational details

The method used in this work is the self-consistent full-potential linearized augmented plane wave (FP-LAPW) [22] as implemented in the ELK code [23], within the limits of LDA [24] and GGA [25] approximations. The study is concerned with the stability of $HgTe$, $CdTe$, $ZnTe$ materials, and their ternary alloys $Hg_{1-x}Cd_xTe$ and $Hg_{1-x}Zn_xTe$ with concentrations $X = 0.25, 0.5, 0.75$, in the zinc blende structure.

The used values of muffin-Tin sphere radii (RMT) in (u.a) are 2.62 for (Hg and Cd) and 2.42 for (Zn and Te). The K points grid in the Brillouin zone is chosen to be $14 \times 14 \times 14$ and the maximum length of (G+K) vectors is fixed so that $8.0/R_{MT} = 1$ a.u $^{-1}$. The self-consistency calculation is stopped when the difference between two successive total energy values is less than 10^{-6} .

Besides the use of LDA and GGA approximations, the

study of electronic properties has required the use of the Tran-Blaha modified Becke-Johnson+LDA potential (TB-mBJLDA) [26], whose formulation is given by:

$$v_{MBJ}^{x,\sigma}(r) = cv_{BR}^{x,\sigma}(r) + (3c - 2) \frac{1}{\pi} \sqrt{\frac{5}{12}} \sqrt{\frac{2t_\sigma(r)}{n_\sigma(r)}}, \quad (1)$$

where c , is the added parameter by Tran and Blaha to the mBJ potential, $v_{BR}^{x,\sigma}$ is the Becke-Rousseln potential, $t_\sigma(r)$ and $n_\sigma(r)$ represent, respectively, the kinetic energy and the electronic densities that are functions of spin. The TB-mBJLDA potential, whose mBJ exchange potential is available in the library interface LIBXC [27], is used in combination with the lattice parameters optimized by the LDA or GGA approximations.

Optical properties were studied using the TB-mBJLDA approximation and a choice of lattice parameter values that guarantee the best gap energies in the range (0-24 eV).

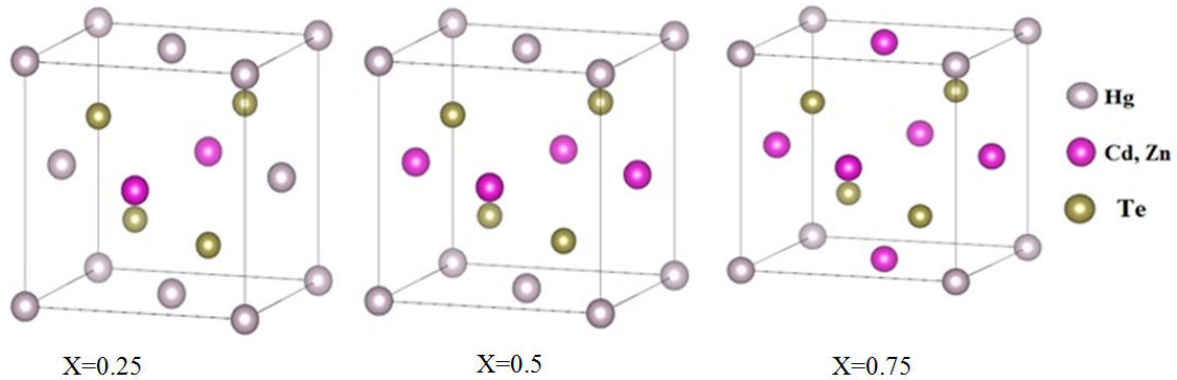
3. Results and discussion

3.1. Structural properties

The equilibrium lattice parameter, the bulk modulus, and the derivative of the bulk modulus of the chosen materials are determined in the zinc blende structure where the binary alloys have the F-43m (2 1 6) space group, where Cd, Zn, or Hg atoms occupy the (0,0,0) position, and Te occupy the (0.25,0.25,0.25); however, the ternary alloys $Hg_{1-x}Cd_xTe$ and $Hg_{1-x}Zn_xTe$ ($x = 0.25, 0.5$ and $x = 0.75$) are the results of the injection of Cd or Zn atoms in the unit cell of $HgTe$. The atomic positions of the different atoms and the different concentrations are reported in Table I; however, the crystal structures are shown in Fig. 1. The variation of the total energy as a function of the lattice volume of each alloy has been represented in the ET-lattice parameter (a) plane. The analytical expressions of these variations have been obtained by the Birch-Murnaghan [28] fit, whose equation of state is:

$$E(V) = E_0 + \frac{9}{8} B_0 V_0 \left(\left[\frac{V_0}{V} \right]^{2/3} - 1 \right)^2 + \frac{9}{16} B_0 (B - 0' - 4) V_0 \left(\left[\frac{V_0}{V} \right]^{2/3} - 1 \right)^3. \quad (2)$$

Table II shows the structural properties of the binary materials: $HgTe$, $CdTe$, and $ZnTe$, which are compared with the available theoretical and experimental data. The lattice parameters obtained by the LDA approximation are close to the experimental values. However, those obtained by the GGA approximation are overestimated. The lattice parameters of $HgTe$, $CdTe$, and $ZnTe$ are in good agreement with the theoretical [11-14-16-42] and experimental data [45-57-58-60]. LDA calculations underestimate values of the lattice constants of $HgTe$, $CdTe$ and, $ZnTe$, by about 0.23% ($HgTe$),

FIGURE 1. Geometrical structures of $\text{Hg}_{1-x}\text{Cd}_x\text{Te}$ and $\text{Hg}_{1-x}\text{Zn}_x\text{Te}$ ($x = 0.25, 0.5$, and 0.75).TABLE I. Atomic positions of $\text{Hg}_{1-x}\text{Cd}_x\text{Te}$ and $\text{Hg}_{1-x}\text{Zn}_x\text{Te}$: ternary alloys.

X	Atomes	Positions
0.25	Hg	(0, 0, 0), (0.5, 0, 0.5), (0.5, 0.5, 0)
	Cd or Zn	(0, 0.5, 0.5)
	Te	(0.25, 0.25, 0.25), (0.75, 0.75, 0.25), (0.75, 0.25, 0.75), (0.25, 0.75, 0.75)
0.5	Hg	(0, 0, 0), (0.5, 0.5, 0)
	Cd or Zn	(0.5, 0, 0.5), (0, 0.5, 0.5)
	Te	(0.25, 0.25, 0.25), (0.75, 0.75, 0.25), (0.75, 0.25, 0.75), (0.25, 0.75, 0.75)
0.75	Hg	(0, 0, 0)
	Cd or Zn	(0.5, 0, 0.5), (0.5, 0.5, 0), (0, 0.5, 0.5)
	Te	(0.25, 0.25, 0.25), (0.75, 0.75, 0.25), (0.75, 0.25, 0.75), (0.25, 0.75, 0.75)

TABLE II. Optimized lattice constant (a), bulk modulus (B) and bulk modulus derivative B' of HgTe, CdTe, and ZnTe in zinc blende structure.

	Parameter	This work		Other works	
		LDA	GGA	Theoretical	Experimental
HgTe	a (Å)	6.445	6.66	6.644 ^a , 6.6385 ^b , 6.458 ^c	6.453 ^d , 6.461 ^g
	B (Gpa)	46.3	32.35	35.57 ^b	42.3i
	B'	5.85	5.78	5.494 ^b	
CdTe	a (Å)	6.487	6.734	6.421 ^c , 6.614 ^b , 6.42 ^m	6.467 ^h , 6.48 ^e
	B (Gpa)	41.91	35.15	42.12 ^b , 44.41 ^m	42.4 ^l
	B'	4.90	3.41	4.99 ^b	6.40 ^l
ZnTe	a (Å)	5.997	6.179	6.174 ^b , 5.98 ^f , 5.99 ^m	6.009 ^l , 6.103 ^j
	B (Gpa)	53.09	41.182	52.21 ^f , 51.62 ^m	51 ^l , 50.50 ^k
	B'	4.80	4.86	4.86 ^f	4.7 ^l , 5.00 ^k

^aRef. [16], ^bRef. [14], ^cRef. [37], ^dRef. [57], ^eRef. [43], ^fRef. [11], ^gRef. [17], ^hRef. [58], ⁱRef. [59], ^jRef. [60], ^kRef. [51], ^lRef. [45], ^mRef. [42].

0.10% (CdTe), and 1.78% (ZnTe) when compared to the experimental values of 6.46 \AA° , 6.48 \AA° , and 6.10 \AA° [17-43-45]. However, GGA calculations overestimate values of the lattice constants of HgTe, CdTe and, ZnTe, by about 3.09% (HgTe), 3.9% (CdTe), and 1.29% (ZnTe) when compared to the experimental values [17-43-45]. Values of the bulk modu-

lus calculated by GGA are smaller than those values found by LDA approximation which are in good agreement with theoretical [11-14-42] and experimental data [59-51-45]. Among the different compounds, it is found that ZnTe has the largest value of bulk modulus (53.09 GPa).

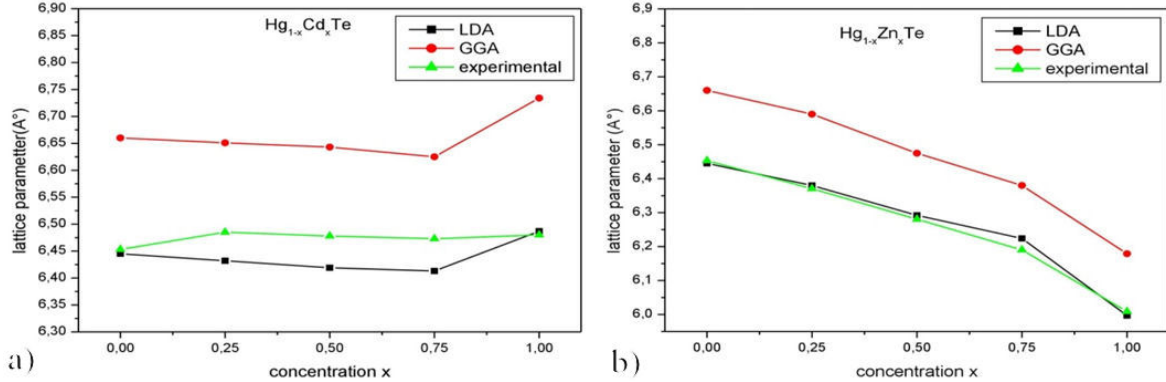


FIGURE 2. Lattice parameter variation of $\text{Hg}_{1-x}\text{Cd}_x\text{Te}$ and $\text{Hg}_{1-x}\text{Zn}_x\text{Te}$ alloys as a function of concentration x (LDA and GGA approximations).

TABLE III. Optimized lattice constant (a), bulk modulus (B) and bulk modulus derivative B' of ternary alloys $\text{Hg}_{1-x}\text{Cd}_x\text{Te}$ and $\text{Hg}_{1-x}\text{Zn}_x\text{Te}$ in zinc blende structure.

	x	Parameter	This work		Other works	
			LDA	GGA	Theoretical	Experimental
$\text{Hg}_{1-x}\text{Cd}_x\text{Te}$	$x = 0.25$	a (Å)	6.432	6,651	6.434 ^a	6.485 ^d
		B (Gpa)	46.77	34.26		
		B'	5.96	4.58		
	$x = 0.50$	a (Å)	6,419	6,643	6.6281 ^b	6.478 ^d
		B (Gpa)	46,62	33.09	35.07 ^b	
		B'	6.19	4.79	4.96 ^b	
	$x = 0.75$	a (Å)	6,413	6,625	6.416 ^a	6.473 ^d
		B (Gpa)	48.38	34.12		
		B'	5.18	5.10		
$\text{Hg}_{1-x}\text{Zn}_x\text{Te}$	$x = 0.25$	a (Å)	6,380	6,590		6.37075 ^c
		B (Gpa)	49.56	36.03		
		B'	4.70	4.57		
	$x = 0.50$	a (Å)	6,292	6,475	6.328 ^b	6.2805 ^c
		B (Gpa)	51.18	41.03	37.85 ^b	
		B'	4.83	4.85	4.765 ^b	
	$x = 0.75$	a (Å)	6,224	6,380		6.1902 ^c
		B (Gpa)	54.91	42,35		
		B'	4.21	4.44		

^aRef. [17], ^bRef. [14], ^cRef. [44], ^dRef. [58].

Results of the optimized equilibrium lattice constant and bulk modulus of $\text{Hg}_{1-x}\text{Zn}_x\text{Te}$ and $\text{Hg}_{1-x}\text{Cd}_x\text{Te}$, obtained by GGA and LDA approximations for various x concentrations, are listed in Table III. For the lattice parameter, it is found that data relative to $\text{Hg}_{1-x}\text{Zn}_x\text{Te}$ and $\text{Hg}_{1-x}\text{Cd}_x\text{Te}$ alloys are in agreement with the theoretical and experimental results [14-17-44-58]. It is observed that an increase in the composition X results in a lattice parameter increase. To the best of our knowledge, there are no bulk modulus experimental data available in the literature for $\text{Hg}_{1-x}\text{Zn}_x\text{Te}$ and $\text{Hg}_{1-x}\text{Cd}_x\text{Te}$ alloys in the range of $X = 0.25$ to $X = 0.75$. Figure 2

shows the plot of the lattice parameter of $\text{Hg}_{1-x}\text{Zn}_x\text{Te}$ and $\text{Hg}_{1-x}\text{Cd}_x\text{Te}$ alloys as a function of concentration X , as calculated by LDA and GGA approximations. It is found that an increase in the concentration x results in a nonlinear variation of the lattice parameter.

3.2. Electronic properties

LDA and GGA approximations are used to compute the band structure of HgTe , CdTe , ZnTe , and their ternary alloys based on Hg . The gap energies obtained from the band structure

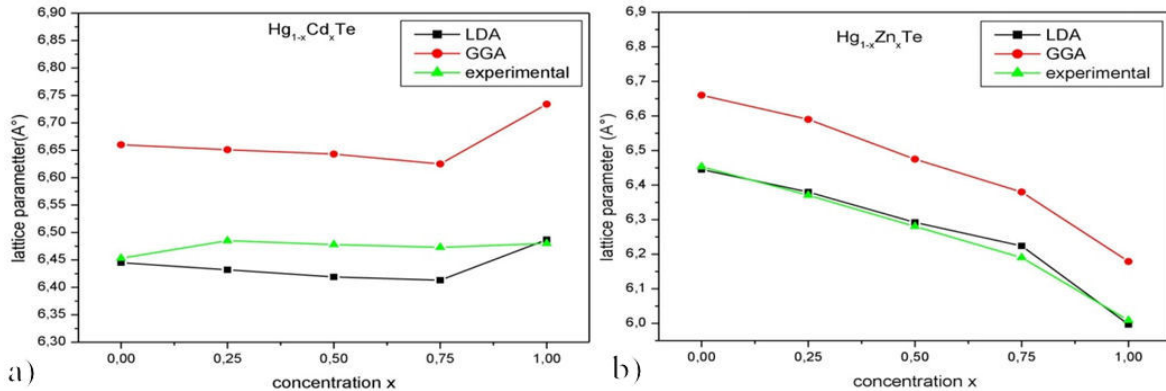


FIGURE 3. Gap energy variation of $Hg_{1-x}Cd_xTe$ and $Hg_{1-x}Zn_xTe$ alloys as function of concentration x (LDA, GGA + TB-mBJLDA and experimental data).

TABLE IV. Gap energy values for binary and ternary alloys of $Hg_{1-x}Cd_xTe$ and $Hg_{1-x}Zn_xTe$ alloys for ($x = 0.0, 0.25, 0.5, 0.75$ and 1), using LDA and GGA approximations.

Alloys	Material	This work			Other works	
		Approximation	Gap energy (eV)	Gap nature	Theoretical (DFT)	Experimental
binary	$HgTe$	LDA	-0.9074		-0.907 ^c	-0.3 ^b
		GGA	-0.9318			
	$CdTe$	LDA	0.501	direct $\Gamma - \Gamma$	0.59 ^a , 0.48 ⁱ	1.606 ^g
		GGA	0.425	direct $\Gamma - \Gamma$		
	$ZnTe$	LDA	1.2661	direct $\Gamma - \Gamma$	1.09 ^a , 1.22 ⁱ	2.38 ^g
		GGA	1.05264	direct $\Gamma - \Gamma$		
	$x = 0.25$	LDA	-0.5241		0.0 ^f	0.22 ^h
		GGA	-0.5579			
$Hg_{1-x}Cd_xTe$	$x = 0.5$	LDA	-0.1576		0.0 ^c	0.592 ^h
		GGA	-0.1997			
	$x = 0.75$	LDA	0.21439	direct $\Gamma - \Gamma$	0.203 ^c	1.06 ^h
		GGA	0.17872	direct $\Gamma - \Gamma$		
	Ternary	$x = 0.25$	-0.51398			0.380 ^e
		GGA	-0.5759			
$Hg_{1-x}Zn_xTe$	$x = 0.5$	LDA	-0.0765		0.24 ^d	0.990 ^e
		GGA	-0.3421			
	$x = 0.75$	LDA	0.3922	direct $\Gamma - \Gamma$		1.621 ^e
		GGA	0.3214	direct $\Gamma - \Gamma$		

^aRef. [11], ^bRef. [56], ^cRef. [16], ^dRef. [14]. ^eRef. [10], ^fRef. [37], ^gRef. [54], ^hRef. [55], ⁱRef. [42].

as well as other theoretical (DFT) and experimental results are reported in Table IV and plotted in Fig. 3. Good agreement is observed between our results and the available theoretical data [11-14-16-42] and far from agreeing with experimental results [10-54-55-56]. The under-estimation of gap energy is one of the problems associated with the use of the DFT (LDA or GGA) while studying electronic properties [18]. Despite the fact of being in good agreement with other theoretical (DFT) studies, the values of band gaps of $HgTe$, $CdTe$, and $ZnTe$ materials differ from the experimental values. Band gaps associated with the ternary alloys $Hg_{1-x}Cd_xTe$ and $Hg_{1-x}Zn_xTe$ are found experimentally to

have low values. In this work, the DFT calculations give very low gap values for $X = 0.75$ and even negative values for $X = 0.25$ and 0.5 . For $Hg_{0.25}Cd_{0.75}Te$, the values of gap energy agree with theoretical data [16,37] and differ slightly for $Hg_{0.75}Cd_{0.25}Te$ and $Hg_{0.5}Cd_{0.5}Te$ compounds. For $Hg_{0.5}Zn_{0.5}Te$, the values of gap energy are different from those reported in Ref. [14], which use the PBE-GGA approximation. To the best of the author's knowledge, no theoretical (DFT) results regarding the gap energies of the band gaps of $Hg_{1-x}Zn_xTe$ at $X = 0.25$ and $X = 0.75$ are found in the literature.

TABLE V. Gap energy values of binary and ternary alloys of $Hg_{1-x}Cd_xTe$ and $Hg_{1-x}Zn_xTe$ alloys ($x = 0.0, 0.25, 0.5, 0.75$, and 1), using TB-mBJLDA potential.

Alloys	Material	This work			Otherworks	
		Lattice parameter	Gap energy (eV)	Gap nature	Theoretical (mBJ or GW)	Experimental
Binary	HgTe	aLDA	-0.01968		-0.701 ^a , -0.03 ^e ,	-0.3 ^h
		aGGA	-0.1649		-0.1 ^f , -0.1 ^g	
	CdTe	aLDA	1.8137	direct $\Gamma - \Gamma$	1.541 ^c , 1.57 ^e	1.606 ⁱ
		aGGA	1.5273	direct $\Gamma - \Gamma$		
	ZnTe	aLDA	2.6981	direct $\Gamma - \Gamma$	2.138 ^c , 2.33 ^f ,	2.38 ⁱ
		aGGA	2.3253	direct $\Gamma - \Gamma$	2.2 ^g	
	$Hg_{1-x}Cd_xTe$	$x = 0.25$	0.4675	direct $\Gamma - \Gamma$	0.39 ^a , 0.22 ^e	0.22 ^b
			0.2670	direct $\Gamma - \Gamma$		
Ternary	$Hg_{1-x}Zn_xTe$	$x = 0.5$	0.892	direct $\Gamma - \Gamma$	0.81 ^a , 0.62 ^e	0.592 ^b
			0.678	direct $\Gamma - \Gamma$		
		$x = 0.75$	1.3486	direct $\Gamma - \Gamma$	1.27 ^a	1.06 ^b
			1.1360	direct $\Gamma - \Gamma$		
	$Hg_{1-x}Zn_xTe$	$x = 0.25$	0.5364	direct $\Gamma - \Gamma$	0.29 ^c	0.380 ^d
			0.3182	direct $\Gamma - \Gamma$		
		$x = 0.5$	1.0729	direct $\Gamma - \Gamma$	0.773 ^c , 0.72 ^g	0.990 ^d
			0.8526	direct $\Gamma - \Gamma$		
	$Hg_{1-x}Zn_xTe$	$x = 0.75$	1.6410	direct $\Gamma - \Gamma$	1.58 ^c , 1.35 ^g	1.621 ^d
			1.4266	direct $\Gamma - \Gamma$		

^aRef. [16], ^bRef. [55], ^cRef. [14], ^dRef. [10], ^eref. [29]. ^fRef. [50], ^gRef. [15], ^hRef[56], ⁱRef. [54].

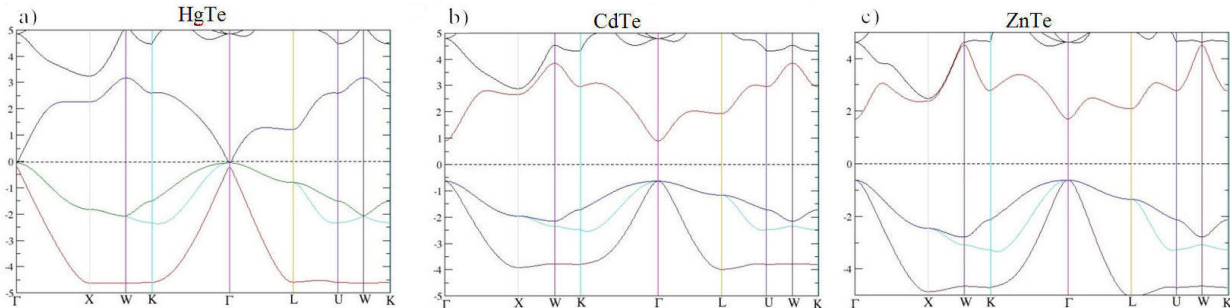
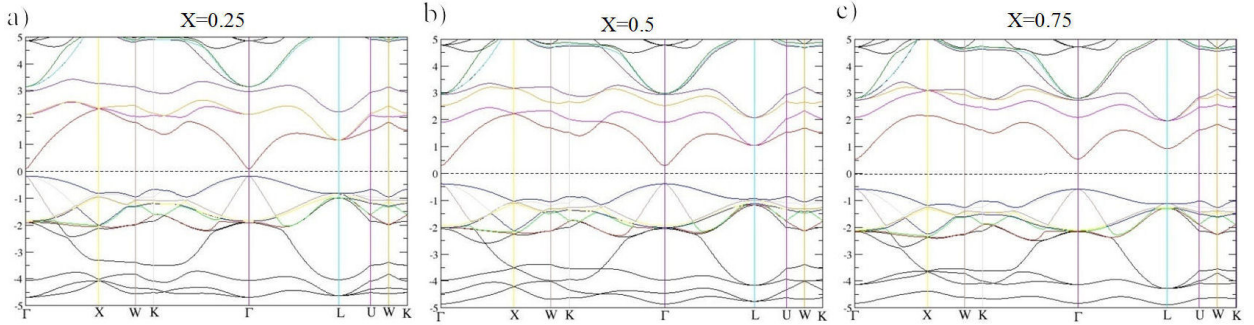
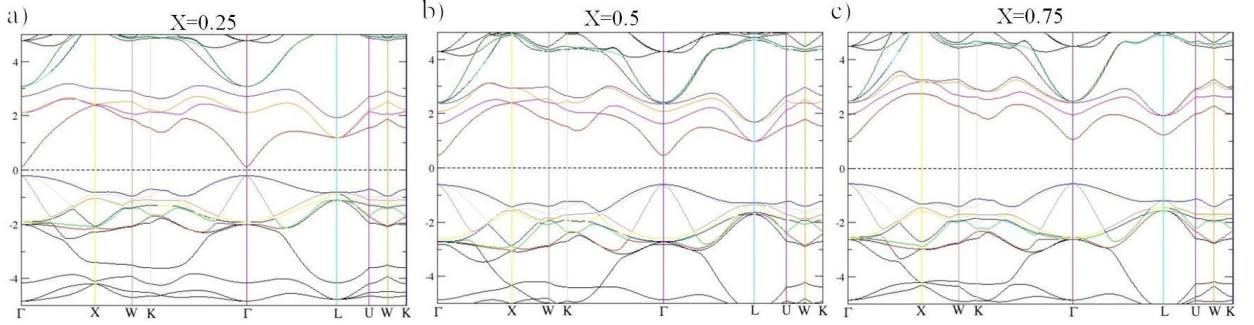


FIGURE 4. Band structure of HgTe, CdTe, and ZnTe using TB-mBJLDA potential and aGGA lattice parameters.

The same study has been extended to compute the band structure by using the Tran and Blaha modified Becke-Johnson potential (TB-mBJ) coupled with the LDA approximation and the insertion of the lattice parameters that have been optimized either by LDA or GGA approaches. The new gap energy values are reported in Table V. Comparison of the electronic properties data leads to ascertain that good agreement is observed between our results and other theoretical studies [14-16-29-15] for $Hg_{1-x}Cd_xTe$ and $Hg_{1-x}Zn_xTe$ alloys for ($X = 0, 0.25, 0.5, 0.75$, and 1).

The gap energy values obtained using the (TB-mBJLDA) approach are, generally, in agreement with the experimental results, which are plotted in Fig. 3, representing a clear im-

provement when compared to the simple DFT (LDA, GGA) results. Given that the gap energy value is very sensitive to small variations in the lattice parameter values, the use of aGGA instead of aLDA in the computation of gap energy of the binary materials HgTe, CdTe, and ZnTe lead to results that are comparable to the experimental data. The same observation is valid for the ternary $Hg_{1-x}Cd_xTe$. However, for $Hg_{1-x}Zn_xTe$, the best gap energies are obtained with aGGA for $Hg_{0.75}Zn_{0.25}Te$ alloy and with aLDA for $Hg_{0.5}Zn_{0.5}Te$ and $Hg_{0.25}Zn_{0.75}Te$ alloys. Figure 4 shows the calculated electronic band structures of the binary materials: HgTe, CdTe, and ZnTe. The valence band maximum (VBMax) and the conduction band minimum (CBMin) for the considered

FIGURE 5. Band structure of $Hg_{1-x}Cd_xTe$ alloy ($x = 0.25, 0.5$, and $x = 0.75$), using TB-mBJLDA and aGGA lattice parameters.FIGURE 6. Band structure of $Hg_{1-x}Zn_xTe$ alloy using TB-mBJLDA and aGGA for $x = 0.25$, and aLDA for $x = 0.5$ and 0.75 .

compounds are located at Γ point. The band gap being direct and located at $\Gamma - \Gamma$. Figure 5 shows plots of the energy bands as calculated with the TB-mBJLDA for $Hg_{1-x}Cd_xTe$. An almost linear increase of the gap energy is observed with increasing Cd concentrations (0.25 to 0.75). Hence, these alloys can be considered semiconductors with direct band gaps at the Γ -point. Plots of the electronic band structure of $Hg_{1-x}Zn_xTe$, for $x = 0.25$ to 0.75, using TB-mBJLDA correction are shown in Fig. 6. An increasing trend of the energy gap is observed with an increasing X.

3.3. Optical properties

The complex dielectric function is the starting point for the computation of the optical properties of different materials. These functions are completely determined by the band structures of the considered materials. Hence, knowledge of the complex dielectric function $\varepsilon(\omega)$ is capable of characterizing the optical response of all materials when subjected to an electromagnetic wave flux [30].

$$\varepsilon(\omega) = \varepsilon_1(\omega) + i\varepsilon_2(\omega), \quad (3)$$

$\varepsilon_1(\omega)$ and $\varepsilon_2(\omega)$ are, respectively, the real and imaginary parts of the dielectric function and ω is the angular frequency. The study covers frequencies corresponding to the energy range [0-24 eV]. Optical constants expressions such as the refractive index $n(\omega)$, the extinction coefficient $k(\omega)$, the energy loss function $L(\omega)$, the absorption coefficient (attenuation) $\alpha(\omega)$, and the reflectivity $R(\omega)$ are expressed in terms of $\varepsilon_1(\omega)$ and $\varepsilon_2(\omega)$ [31-32-33] as follows:

$$n(\omega) = \frac{1}{\sqrt{2}} \left(\sqrt{\varepsilon_1^2(\omega) + \varepsilon_2^2(\omega)} + \varepsilon_1(\omega) \right)^{1/2}, \quad (4)$$

$$k(\omega) = \frac{1}{\sqrt{2}} \left(\sqrt{\varepsilon_1^2(\omega) + \varepsilon_2^2(\omega)} - \varepsilon_1(\omega) \right)^{1/2}, \quad (5)$$

$$L(\omega) = \frac{\varepsilon_2(\omega)}{(\varepsilon_1^2(\omega) + \varepsilon_2^2(\omega))} \quad (6)$$

$$\alpha(\omega) = 2 \frac{\omega}{c} k(\omega) = \sqrt{2} \frac{\omega}{c} \left(\sqrt{\varepsilon_1^2(\omega) + \varepsilon_2^2(\omega)} - \varepsilon_1(\omega) \right)^{1/2}, \quad (7)$$

$$R(\omega) = \frac{(n-1)^2 + k^2}{(n+1)^2 + k^2}. \quad (8)$$

In Figs. 7 and 8, the spectrums of the real and imaginary parts of the dielectric function are represented. They summarize the optical processes resulting from the interaction of an electromagnetic wave with a given material. Each material exhibits a Mie resonance when $\varepsilon_1 \gg 1$ and $\varepsilon_2 \ll 1$, and a metallic character when $\varepsilon_1(\omega) < 0$. Plasmon resonance is observed when $\varepsilon_1 < 0$ and $\varepsilon_2 \ll 1$. The peaks in the imaginary part spectrum match the inter-band transition [34-35]. The semi-metal HgTe possesses a Mie resonance in the range mid-infrared- short-wave infrared (MWIR-SWIR) and a Plasmon resonance in the ultraviolet (UV). In the energy ranges (4.15 – 4.49 eV) and (6.15 – 14.57 eV), $\varepsilon_1(\omega)$ becomes negative. The first and main peaks of $\varepsilon_2(\omega)$ fall,

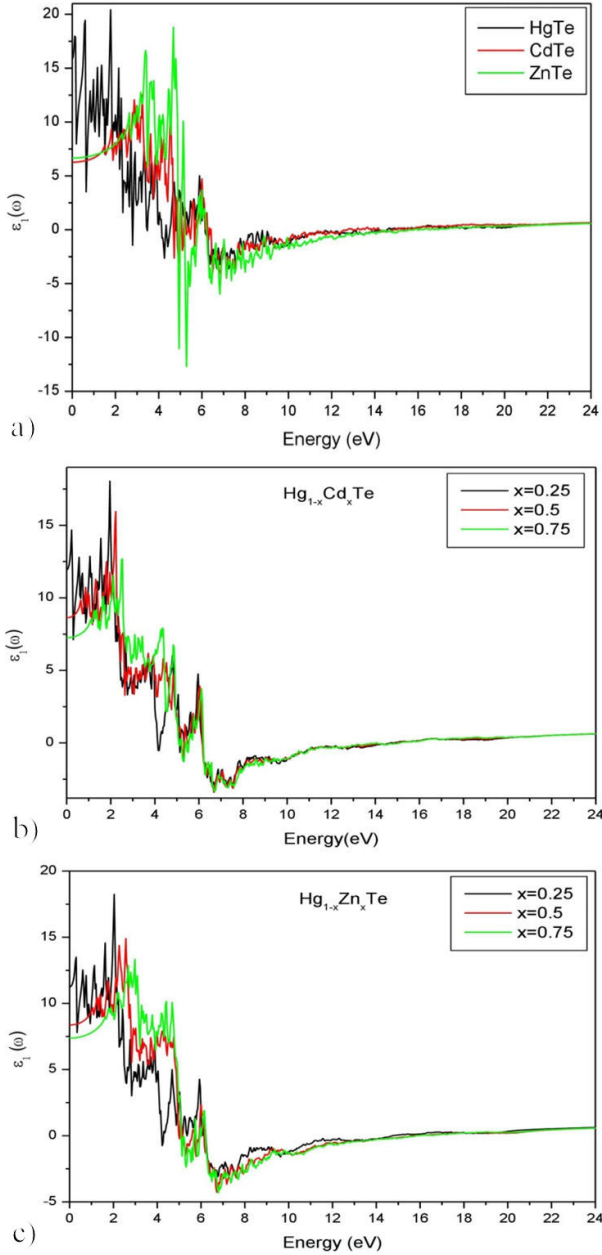


FIGURE 7. Spectrum of the real part of the dielectric function of $Hg_{1-x}Cd_xTe$ and $Hg_{1-x}Zn_xTe$ alloys for ($x = 0, 0.25, 0.5, 0.75$ and 1).

respectively, at energies 0.15 eV and 2.30 eV. A Mie resonance is associated with the CdTe material, in the visible-infrared (V-IR) range, and a Plasmon resonance in the ultraviolet (UV). In the three energy ranges: $(4.87 - 5.47$ eV), $(6.26 - 12.72$ eV) and $(14.23 - 14.80$ eV), $\varepsilon_1(\omega)$ becomes negative. The first and main peaks of $\varepsilon_2(\omega)$ are observed, respectively, at energies 1.85 eV and 4.68 eV. The ZnTe possesses a Mie resonance in the infrared-ultraviolet (IR-UV) range and a Plasmon resonance in the ultraviolet (UV). In the $(5.21-5.77$ eV) and $(6.22 - 16.04$ eV) energy intervals, $\varepsilon_1(\omega)$ changes to a negative sign. The first and main peaks of $\varepsilon_2(\omega)$ appear respectively at energies 2.68 eV and 4.90 eV. For the

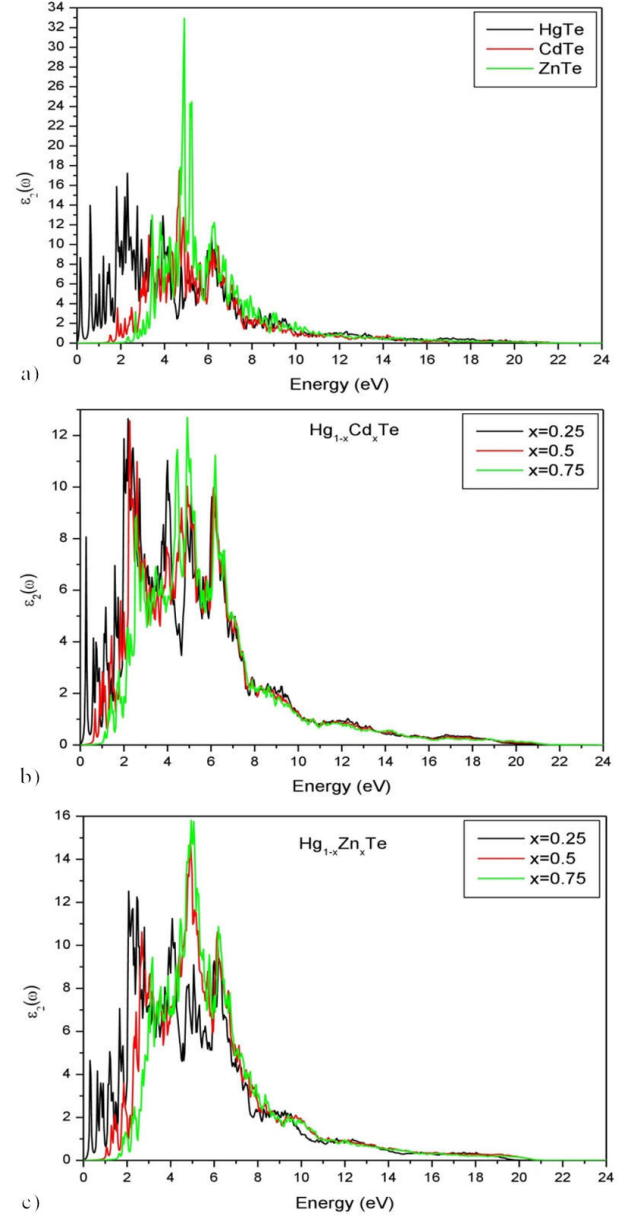


FIGURE 8. Spectrum of the imaginary part of the dielectric function of $Hg_{1-x}Cd_xTe$ and $Hg_{1-x}Zn_xTe$ alloys for ($x = 0, 0.25, 0.5, 0.75$ and 1).

ternary alloy $Hg_{1-x}Cd_xTe$, ($x = 0.25$), the Mie resonance is located in the far-infrared- short-wave infrared (FIR-SWIR) range. However, the Plasmon resonance is found in the ultra-violet (UV) zone. $\varepsilon_1(\omega)$ changes sign in the energy range $(6.15 - 14.64$ eV). The first peak and the main peak of $\varepsilon_2(\omega)$ are observed, respectively, at 0.26 eV and 2.18 eV. For the case of $x = 0.5$, the Mie resonance is observed in the Far Infrared- short-wave Infrared (FIR-SWIR) range. However, the Plasmon resonance shows up in the Ultraviolet (UV) range. Negative values of $\varepsilon_1(\omega)$ are observed in the energy interval $(6.19 - 14.98$ eV). The first and main peaks of $\varepsilon_2(\omega)$ correspond, respectively, to 0.67 eV and 2.26 eV. For $x = 0.75$ the Mie resonance is found in the whole infrared

(IR) range, and the Plasmon resonance is located in the ultra-violet (UV) range. $\varepsilon_1(\omega)$ changes sign in two energy ranges: (5.09 – 5.51 eV) and (6.22 – 15.10 eV). The energies associated with the first and main peaks of the imaginary part $\varepsilon_2(\omega)$ are found at 1.39 eV and 4.90 eV, respectively. For the second ternary alloy $\text{Hg}_{1-x}\text{Zn}_x\text{Te}$, and for $X = 0.25$ concentration, the Mie resonance is found in the Far infrared- short-wave infrared (FIR-SWIR) region and the Plasmon resonance in the ultraviolet (UV). The real part of $\varepsilon_1(\omega)$, shifts to negative values in the region (6.22 – 14.64 eV). The first and main peaks of $\varepsilon_2(\omega)$, are found at 0.30 eV and 2.03 eV, respectively. For $X = 0.5$, the material shows a Mie resonance in the Far-infrared- near-infrared (FIR-NIR) region and a Plas-

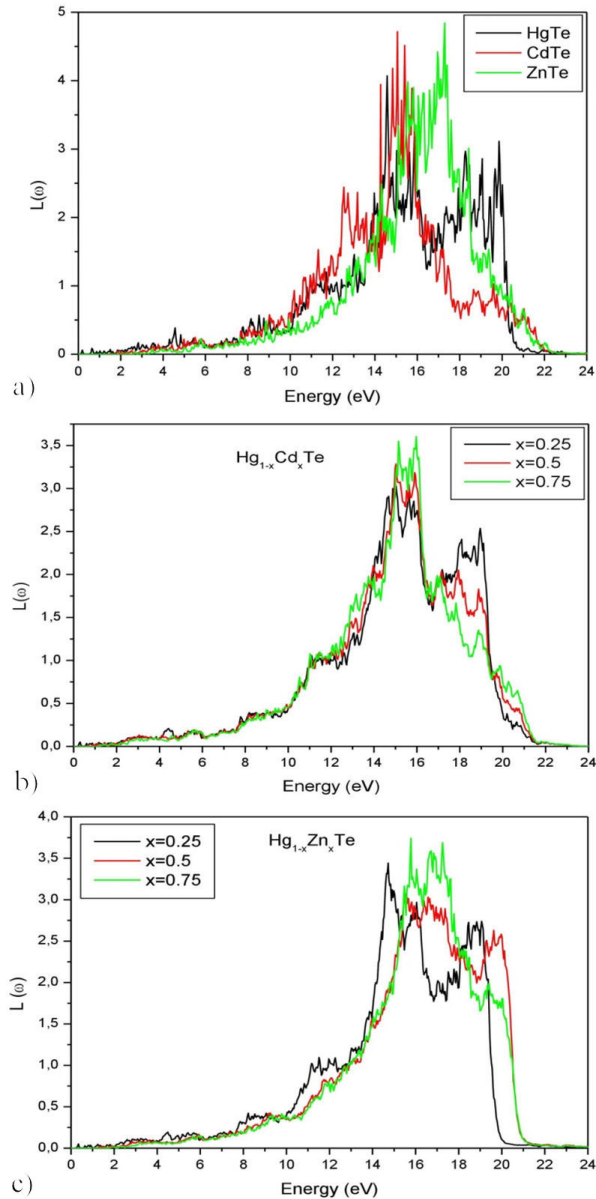


FIGURE 9. Energy loss function $L(\omega)$ of $\text{Hg}_{1-x}\text{Cd}_x\text{Te}$ and $\text{Hg}_{1-x}\text{Zn}_x\text{Te}$ alloys for ($x = 0, 0.25, 0.5, 0.75$ and 1) as a function of energy.

mon resonance in the ultraviolet C (UVC). In the energy range (6.15 - 15.59 eV), the real part of $\varepsilon_1(\omega)$, becomes negative. The first and main peaks of $\varepsilon_2(\omega)$, are found at 1.43 eV and 4.90 eV, respectively. For the case of $X = 0.75$, the Mie resonance is observed in the visible-infrared (V-IR) region, while the Plasmon resonance is found in the ultraviolet C (UVC). In the (5.09 – 6 eV) and (6.22 – 15.74 eV) energy zones, the real part of the dielectric function shifts to negative values. The first and main peaks of $\varepsilon_2(\omega)$ show up at energy 1.92 eV and 4.94 eV. The obtained results are in agreement with those reported in Ref. [16] for the case of the $\text{Hg}_{1-x}\text{Cd}_x\text{Te}$ alloy, and with those reported in Ref. [48] for the ZnTe material. For $\text{Hg}_{1-x}\text{Zn}_x\text{Te}$, the results of dielectric function are in agreement with [15] except for $X = 0.25$ and 0.5, where the imaginary part spectrum differs slightly. In the literature, data regarding the optical properties of the studied materials have been scarce.

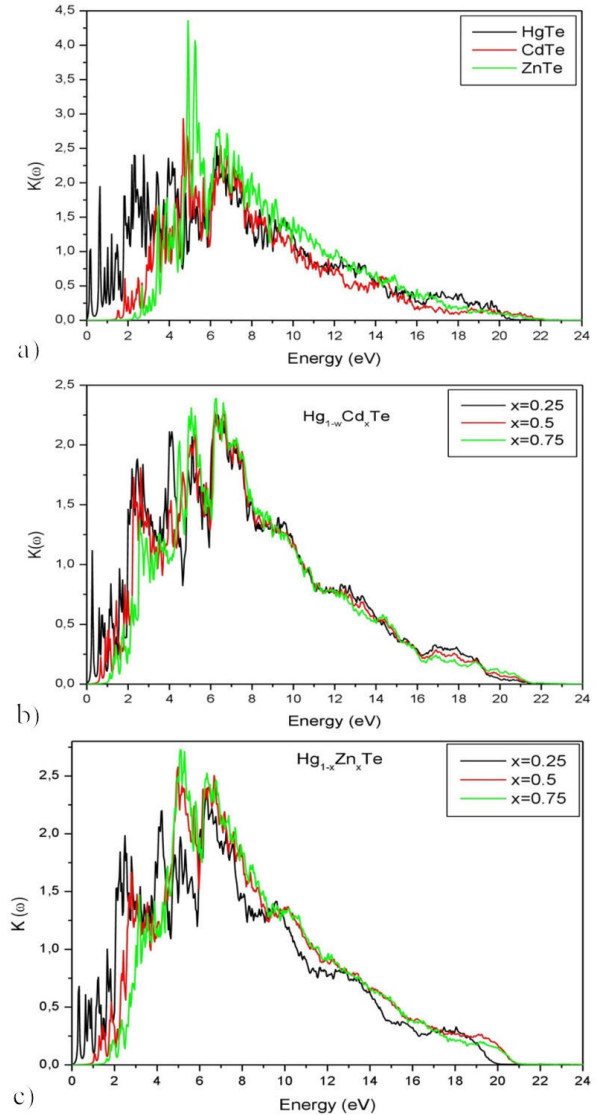


FIGURE 10. Extinction coefficient of $\text{Hg}_{1-x}\text{Cd}_x\text{Te}$ and $\text{Hg}_{1-x}\text{Zn}_x\text{Te}$ alloys for ($x = 0, 0.25, 0.5, 0.75$ and 1) as a function of energy.

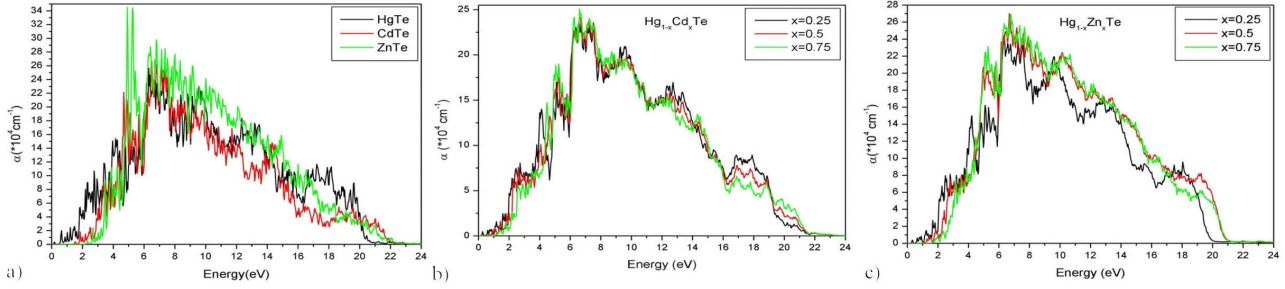


FIGURE 11. Absorption coefficient $\alpha(\omega)$ of $\text{Hg}_{1-x}\text{Cd}_x\text{Te}$ and $\text{Hg}_{1-x}\text{Zn}_x\text{Te}$ alloys for ($x = 0, 0.25, 0.5, 0.75, 1$) as a function of energy.

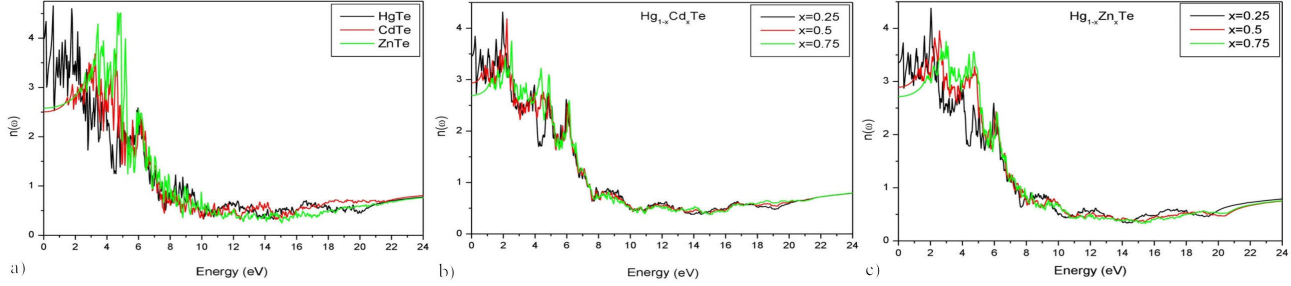


FIGURE 12. Refractive index of $\text{Hg}_{1-x}\text{Cd}_x\text{Te}$ and $\text{Hg}_{1-x}\text{Zn}_x\text{Te}$ alloys for ($x = 0, 0.25, 0.5, 0.75$ and 1) as a function of energy.

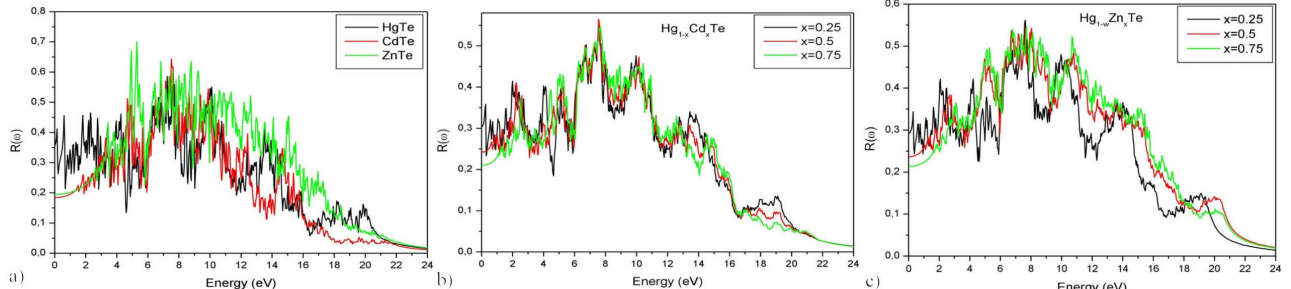


FIGURE 13. Reflectivity $R(\omega)$ of $\text{Hg}_{1-x}\text{Cd}_x\text{Te}$ and $\text{Hg}_{1-x}\text{Zn}_x\text{Te}$ alloys for ($x = 0, 0.25, 0.5, 0.75$ and 1) as a function of energy.

TABLE VI. Static dielectric function $\varepsilon_1(0)$, refractive index $n(0)$ and reflectivity $R(0)$ of $\text{Hg}_{1-x}\text{Cd}_x\text{Te}$ and $\text{Hg}_{1-x}\text{Zn}_x\text{Te}$ alloys, using TB-mBJLDA potential.

Alloys	Material	$\varepsilon_1(0)$		$n(0)$		$R(0)$	
		This work	Other works	This work	Other works	This work	Other works
Binary	HgTe	15.85	16.9 ^d , 15.35 ^j	3.98	3.7 ^e	4.51g	0.358
	CdTe	6.27	6.7c	2.50	2.55e	3.26h	0.184
	ZnTe	6.65	6.75b, 7.1j	2.58	2.5b	4.5g	0.194
	$\text{Hg}_{1-x}\text{Cd}_x\text{Te}$	$x=0.25$	11.93	15.35c	-	3.30e	0.303
	$\text{Hg}_{1-x}\text{Cd}_x\text{Te}$	$x=0.5$	8.62	10.41c	-	3.00e	0.242
Ternary	$\text{Hg}_{1-x}\text{Cd}_x\text{Te}$	$x=0.75$	7.25	7.53c	-	2.74e	0.210
	$\text{Hg}_{1-x}\text{Zn}_x\text{Te}$	$x=0.25$	11.71	-	-	3.422	-
	$\text{Hg}_{1-x}\text{Zn}_x\text{Te}$	$x=0.5$	8.36	-	-	2.892	-
	$\text{Hg}_{1-x}\text{Zn}_x\text{Te}$	$x=0.75$	7.37	-	-	2.716	-
							0.213

^aRef. [53], ^bRef. [31], ^cRef. [37], ^dRef. [52], ^eRef. [29], ^fRef. [46], ^gRef. [40], ^hRef. [47], ⁱRef. [41], ^jRef[15].

The loss of electron's energy, when moving in a given material, is defined by the energy loss function $L(\omega)$ given in Fig. 9, for which the main peaks are associated with the Plasmon frequencies ω_p ($E_{\text{plasmon}} = \hbar X \omega_p$, ω_p [14-36]). For the binary materials HgTe, CdTe, and ZnTe, the first peaks of $L(\omega)$ are observed at 4.56 eV, 5.51 eV, and 7.87 eV, respectively. The main peaks are situated at 14.57 eV, 15.06 eV, and 17.29 eV, respectively. In the case of the ternary alloy $\text{Hg}_{1-x}\text{Cd}_x\text{Te}$, the first peaks of $L(\omega)$ appear at 4.41 eV, 5.62 eV and 5.73 eV for $X = 0.25, 0.5, 0.75$, respectively, while the main peaks are observed at 15.02 eV, 15.02 eV and 15.97 eV, respectively. The first peaks of $\text{Hg}_{1-x}\text{Zn}_x\text{Te}$ for $X = 0.25, 0.5$, and 0.75 appear at 4.41 eV, 5.92 eV, and 8.30 eV, respectively, while the main peaks are observed at 14.57 eV, 15.51 eV, and 15.78 eV, respectively. For each alloy and any energy less than the first peak energy, there is no loss of electron energy. For $x = 0, 0.25, 0.5, 0.75$, and 1.0, the energies associated with the Plasmon frequencies are found to be greater than those cited in the work of Gang Wang *et al.*, [37] in the case of $\text{Hg}_{1-x}\text{Cd}_x\text{Te}$, and in the work of Qing-Fang Li *et al.*, [38] for the ZnTe material. It should be reminded that, in these studies, the computation of the dielectric func-

tion was done for gap energies smaller than those used in our work. For HgTe, the results of $L(\omega)$ agree with the data reported in [39]. For $\text{Hg}_{1-x}\text{Zn}_x\text{Te}$, the energies associated with the main peaks of $L(\omega)$ are in good agreement with [15].

The absorption coefficient $\alpha(\omega)$ is related to the extinction coefficient $K(\omega)$ (Eqs. 5 and 7) and accounts for the average distance traveled by photons, before being absorbed in the material [35]. For the binary alloys, absorption starts from energy values: 1.2 eV [HgTe], 1.85 eV [CdTe] and 2.68 eV [ZnTe]. It reaches maximal values at 6.30 eV [HgTe], 7.13 eV [CdTe] and 4.90 eV [ZnTe]. These results are comparable to those cited in [49]. For the ternary alloy $\text{Hg}_{1-x}\text{Cd}_x\text{Te}$ ($X=0.25, 0.5$ and 0.75), the absorption starts at 1.58 eV, 1.43 eV and 1.77 eV, respectively. It reaches maximum values at 6.60 eV, 6.64 eV and 6.60 eV. In the case of the ternary alloy $\text{Hg}_{1-x}\text{Zn}_x\text{Te}$ ($X = 0.25, 0.5$ and 0.75), the absorption starts at 1.20 eV, 1.85 eV and 2.34 eV, respectively. It becomes maximal at 6.30 eV, 6.68 eV, and 6.75 eV. Extinction coefficient and absorption coefficient spectrum are reported in Figs. 10 and 11, respectively. The absorption coefficients relative to the ternary alloy $\text{Hg}_{1-x}\text{Zn}_x\text{Te}$ are found to agree with [15]. For $\text{Hg}_{1-x}\text{Cd}_x\text{Te}$ alloy, the absorption coefficient

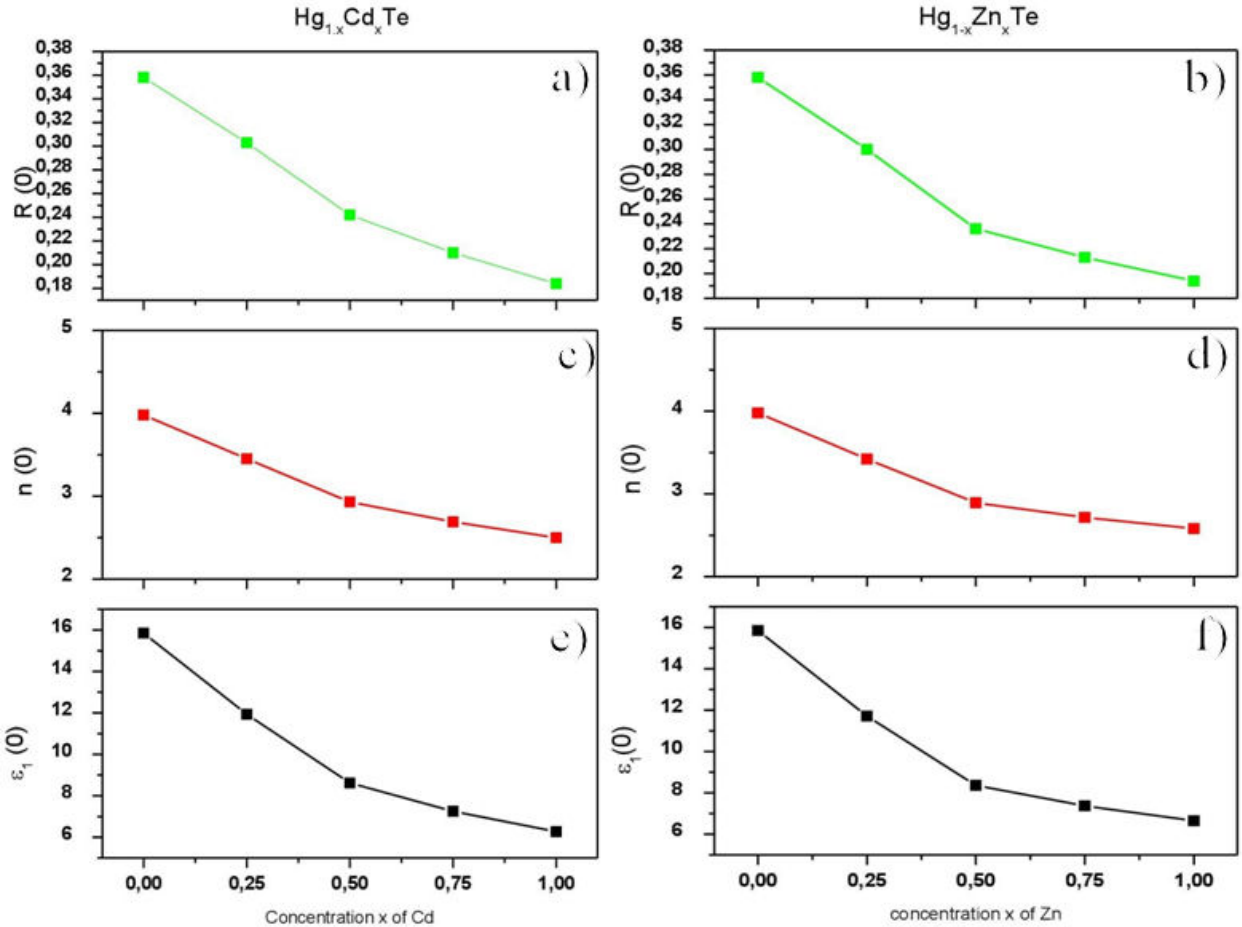


FIGURE 14. Variation of the dielectric constant, the refractive index and the reflectivity of $\text{Hg}_{1-x}\text{Cd}_x\text{Te}$ and $\text{Hg}_{1-x}\text{Zn}_x\text{Te}$ alloys as a function of concentration x at $(\omega = 0)$.

spectrums, as reported in this work, are published for the first time and may constitute data to be compared within future works.

The refractive index $n(\omega)$ plot presented in Fig. 12 and that of the reflection coefficient $R(\omega)$ in Fig. 13 of the based HgTe ternary alloys shows a decreasing trend as a function of Cd and Zn concentrations. For a given frequency ω and for the binary materials: HgTe, CdTe, and ZnTe, the maximal values of the reflection coefficient fall into the Ultraviolet C (UVC) region. The same conclusion is valid for all concentrations X of Cd in the $Hg_{1-x}Cd_xTe$ and of Zn in the $Hg_{1-x}Zn_xTe$ materials.

The refractive index $n(\omega)$, the reflection coefficient $R(\omega)$, and the static value $\varepsilon_1(0)$, associated with different alloys, are reported in Table VI and are represented, in Fig. 14, as functions of concentration x . The values of $\varepsilon_1(0)$ for CdTe, ZnTe, and $Hg_{0.25}Cd_{0.75}Te$ are in agreement with the results of other theoretical works; however, for HgTe, ZnTe, $Hg_{0.75}Cd_{0.25}Te$ and $Hg_{0.5}Cd_{0.5}Te$ materials $\varepsilon_1(0)$ differ sensibly from the results reported in Refs. [31-37-15-52]. It should be noted that for CdTe and ZnTe, the values of $\varepsilon_1(0)$ are in disagreement with the experimental results in Ref. [46-47]. The calculated refractive index is in good agreement with other theoretical [29-31] and experimental [40-41-47] results for HgTe, CdTe, $Hg_{0.5}Cd_{0.5}Te$ and $Hg_{1-x}Zn_xTe$ (for $X = 0.25, 0.5$ and 0.75). For ZnTe, the value of $n(0)$ is in agreement with other theoretical results [31] but differs from the experimental data [40]. Since no theoretical or experimental studies have been carried out on the optical properties, namely refractive index and reflection index of $Hg_{0.75}Cd_{0.25}Te$ and $Hg_{0.25}Cd_{0.75}Te$, no conclusions can be drawn on the validity of our results, for they are still open to experimental verification.

4. Conclusion

In summary, the structural, electronic, and optical properties of $Hg_{1-x}Cd_xTe$ and $Hg_{1-x}Zn_xTe$ alloys were inves-

tigated using the full-potential linearized augmented plane wave (FP-LAPW). The study of structural properties of $Hg_{1-x}Cd_xTe$ and $Hg_{1-x}Zn_xTe$ materials, as done in this work, has confirmed that results obtained by the LDA approximation are better than those obtained by the GGA approach. The bulk modulus of $Hg_{1-x}Zn_xTe$ is greater than those of $Hg_{1-x}Cd_xTe$ alloys. The gap energies deduced from the band structures are underestimated by the LDA and the GGA for the two ternary alloys; however, they compare well to the experimental results when the mBJ-LDA potential is used. The same potential mBJ-LDA gives different values of gaps depending on the use of the lattice parameter aLDA calculated by the LDA approximation, or the use of the lattice parameter aGGA calculated by the GGA approximation. For all alloys, the coupling of mBJ-LDA potential with the lattice parameter aGGA, gives better results except for the case of $Hg_{0.5}Zn_{0.5}Te$ and $Hg_{0.25}Zn_{0.75}Te$, where the use of the lattice parameter aLDA is preferable. For the binary and ternary alloys, the electronic properties, evaluated under either the LDA, GGA, or TB-mBJLDA potential schemes, are found to be those of semiconductors with direct band gaps at the Γ -point. The critical points of the optical constant spectrum (first peaks, main peaks, etc.) calculated from the dielectric function of $Hg_{1-x}Cd_xTe$ and $Hg_{1-x}Zn_xTe$ alloys are distinct. This distinction can be attributed to the difference in gap energies and the nature of the elements composing the different materials. In conclusion, one can say that the two ternary alloys possess comparable optical properties (refractive index, dielectric constant, and reflectivity). Results relative to the optical properties of the studied compounds could bear practical importance; especially, in applications such as microelectronic, optoelectronic, solar cell, and nuclear systems.

-
1. D. R. Yakovlev and W. Ossau, Magnetic Polarons, in *Introduction to the Physics of Diluted Magnetic Semiconductors*, edited by J. Kossut and J. A. Gaj (Springer-Verlag, Berlin, 2010); pp 18-19. DOI 10.1007/978-3-642-15856-8
 2. ESPI Metals. Mercury Zinc Telluride (HgZnTe) Semiconductors. AZoM. <https://www.azom.com/article.aspx?ArticleID=8467>. viewed 20 November 2019.
 3. M. Diakides, J. D. Bronzino, and D. R. Peterson, eds. Medical infrared imaging: principles and practices. (CRC press, 2012). <https://doi.org/10.1201/b12938pp1.1-1.15>
 4. Williams, Philip C, and Susan G. Stevenson. Near-infrared reflectance analysis: food industry applications. *Trends Food Sci. Technol.* **1** (1990) 44. [https://doi.org/10.1016/0924-2244\(90\)90030-3](https://doi.org/10.1016/0924-2244(90)90030-3)
 5. R. R. Hampton, Applied Infrared Spectroscopy in the Rubber Industry, *Rubber Chem. Technol.* **45** (1972) 46, <https://doi.org/10.5254/1.3544726>
 6. C. Corsi, Infrared: A Key Technology for Security Systems, *Adv. Opt. Technol.* vol. **2012**, Article ID 838752, (2012). <https://doi.org/10.1155/2012/838752>
 7. R.S. Hansen , Modeling of the nonlinear response of the intrinsic HgCdTe photoconductor by a two-level rate equation with a finite number of carriers available for photoexcitation, *Appl. Opt.* **42** (2003) 4819. doi: 10.1364/ao.42.004819.
 8. N. Romeo V. Canevari L. Zini C. Spaggiari, HgCdTe thin films for solar cells application prepared by multisource evaporation, *Thin Solid Films*, **157** (1988) 175. [https://doi.org/10.1016/0040-6090\(88\)90001-6](https://doi.org/10.1016/0040-6090(88)90001-6)

9. Rogalski, Antony. HgCdTe infrared detector material: history, status and outlook. *Rep. Prog. Phys.* **68** (2005) 2267. [urlhttps://doi.org/10.1088/0034-4885/68/10/R01](https://doi.org/10.1088/0034-4885/68/10/R01)
10. A. Rogalski, $Hg_{1-x}Z_xTe$ As a potential infrared detector material *Prog. Quant. Electr.* **13** (1989) 299. [https://doi.org/10.1016/0079-6727\(89\)90008-6](https://doi.org/10.1016/0079-6727(89)90008-6)
11. M. Boucharef, *et al.* First-principles study of the electronic and structural properties of $(CdTe)_n/(ZnTe)_n$ superlattices. *Superlattices Microstruct.* **75** (2014) 818. <https://doi.org/10.1016/j.spmi.2014.09.014>
12. F. Hassan, El Haj, *et al.* Ab initio study of the fundamental properties of $HgSe$, $HgTe$ and their $HgSe_xTe_{1-x}$ alloys. *Phys. Scr.* **84.6** (2011) 065601. <https://doi.org/10.1088/0031-8949/84/6/065601>
13. M. Debbarma *et al.*, Density Functional Calculations of Elastic and Thermal Properties of Zinc-Blende Mercury-Cadmium-Chalcogenide Ternary Alloys. *Met. Mater. Int.* (2020). <https://doi.org/10.1007/s12540-020-00778-7>
14. F. Kadari, *et al.* First-principles study of the structural, electronic and optical properties of the cubic triangular quaternary $Zn_xCd_yHg_{1-x-y}Te$ alloys under hydrostatic pressure. *Chin. J. Phys.* **59** (2019) 209. <https://doi.org/10.1016/j.cjph.2019.02.016>
15. A. Laref, *et al.* Compositional and spin-orbit control on the electronic structure and optical characteristics of $Zn-HgTe$ alloys using mBJ-GGA approach. *J. Mater. Sci.* **52.12** (2017) 7039-7057. <https://doi.org/10.1007/s10853-017-0937-5>
16. S. Al-Rajoub, and B. Hamad, Theoretical investigations of the structural, electronic and optical properties of $Hg_{1-x}Cd_xTe$ alloys. *Philos Mag.* **95.22** (2015) 2466-2481. <https://doi.org/10.1080/14786435.2015.1061219>
17. B.V. Robouch *et al.*, Ion distribution preferences in ternary crystals $Zn_xCd_{1-x}Te$, $Zn_{1-x}Hg_xTe$ and $Cd_{1-x}Hg_xTe$. *Eur. Phys. J. B* **84.2** (2011) 183-195. <https://doi.org/10.1140/epjb/e2011-20575-1>
18. A. Morales-García, R. Valero, and F. Illas, An empirical, yet practical way to predict the band gap in solids by using density functional band structure calculations. *J. Phys. Chem C.* **121** (2017): 18862-18866. [10.1021/acs.jpcc.7b07421](https://doi.org/10.1021/acs.jpcc.7b07421).
19. S. Belhadj, B. Lagoun, M. Benabdallah Taouti, S. Khenchouli, A. Benghia, and D. Benbental. TB-mBJ calculation of structural, electronic and optical properties of two monovalent iodates AlO_3 ($A = Ti, \alpha-Rb$). *Chin. J. Phys.* **59** (2019) 10-20. <https://doi.org/10.1016/j.cjph.2019.02.019>
20. J. A. Camargo-Martínez, and R. Baquero, Performance of the modified Becke-Johnson potential for semiconductors. *Phys. Rev. B.* **86.19** (2012) 195106. <https://doi.org/10.1103/PhysRevB.86.195106>
21. D. Koller, F. Tran, and P. Blaha, Merits and limits of the modified Becke-Johnson exchange potential *Phys. Rev. B.* **83.19** (2011) 195134. <https://doi.org/10.1103/PhysRevB.83.195134>
22. T. Takeda, Linear methods for fully relativistic energy-band calculations. *J. Phys. F: Met. Phys.* **9.5** (1979) 815. <https://doi.org/10.1088/0305-4608/9/5/009>
23. Elk version 5.2.14, <http://elk.sourceforge.net/>.
24. J. P. Perdew, E. R. McMullen, and Alex Zunger, Density-functional theory of the correlation energy in atoms and ions: a simple analytic model and a challenge. *Phys. Rev. A.* **23.6** (1981) 2785. <https://doi.org/10.1103/PhysRevA.23.2785>
25. Perdew, John P., Kieron Burke, and Matthias Ernzerhof. Generalized gradient approximation made simple. *Phys. Rev. Lett.* **77.18** (1996) 3865. <https://doi.org/10.1103/PhysRevLett.77.3865>
26. Meinert, Markus. Modified Becke-Johnson potential investigation of half-metallic Heusler compounds. *Phys. Rev. B.* **87.4** (2013) 045103. <https://doi.org/10.1103/PhysRevB.87.045103>
27. Marques, Miguel AL, Micael JT Oliveira, and Tobias Burnus. Libxc: A library of exchange and correlation functionals for density functional theory. *Comput. Phys. Commun.* **183.10** (2012) 2272. <https://doi.org/10.1016/j.cpc.2012.05.007>
28. Birch, Francis. Finite elastic strain of cubic crystals. *Phys. Rev.* **71.11** (1947) 809. <https://doi.org/10.1103/PhysRev.71.809>
29. San-Dong, Guo, and Liu Bang-Gui. Density-functional theory investigation of energy gaps and optical properties of $Hg_{1-x}Cd_xTe$ and $In_{1-x}Ga_xAs$. *Chin. Phys. B.* **21.1** (2012) 017101. <https://doi.org/10.1088/1674-1056/21/1/017101>
30. Qi-Jun, Liu, Zhang Ning-Chao, Liu Fu-Sheng, and Liu Zheng-Tang. Structural, electronic, optical, elastic properties and Born effective charges of monoclinic HfO_2 from first-principles calculations. *Chin. Phys. B.* **23**, no. 4 (2014): 047101. <https://doi.org/10.1088/1674-1056/23/4/047101>
31. Korozlu, Nurettin, K. Colakoglu, and E. Deligoz. Structural, electronic, elastic and optical properties of $cdxzn_{1-x}te$ mixed crystals. *Journal of Physics: Condensed Matter* **21.17** (2009) 175406. <https://doi.org/10.1088/0953-8984/21/17/175406>
32. Ilyas, Bahaa M., and Badal H. Elias. A theoretical study of perovskite $CsXCl_3$ ($X = Pb, Cd$) within first principles calculations. *Physica B Condens* **510** (2017) 60-73. <https://doi.org/10.1016/j.physb.2016.12.019>
33. Zaari, H., M. Boujnah, A. El Hachimi, A. Benyoussef, and A. El Kenz. Optical properties of $ZnTe$ doped with transition metals (Ti, Cr and Mn). *Opt Quant Electron.* **46** (2014) 75-86. <https://doi.org/10.1007/s11082-013-9708-y>
34. Toudert, Johann, and Rosalía Serna. Interband transitions in semi-metals, semiconductors, and topological insulators: a new driving force for plasmonics and nanophotonics. *Opt. Mater. Express.* **7** (2017) 2299-2325. <https://doi.org/10.1364/OME.7.002299>
35. Ali, M. A., M. Anwar Hossain, M. A. Rayhan, M. M. Hossain, M. M. Uddin, Md Roknuzzaman, Ken Ostrikov, A. K. M. A. Islam, and S. H. Naqib. First-principles study of elastic, electronic, optical and thermoelectric properties of newly synthesized $K_2Cu_2GeS_4$ chalcogenide. *J. Alloys Compd.* **781**: 37-46(2019). <https://doi.org/10.1016/j.jallcom.2018.12.035>

36. Mendi, R. Taghavi, S. M. Elahi, and M. R. Abolhassani. First-principles investigation of the structural, electronic and optical properties of V-doped single-walled ZnO nanotube (8, 0).*MOD PHYS LETT B.* 28:17: 1450139(2014). <https://doi.org/10.1142/S0217984914501395>
37. Wang, Gang, Song Wu, Zhaohua Geng, Songyou Wang, Liangyao Chen, and Yu Jia. First-principles study on the electronic structures and the optical properties of Hg_{1-x}Cd_xTe. *J KOREAN PHYS SOC.* 56, no. 41 : 1307-1310(2010). DOI: 10.3938/jkps.56.1307
38. Li, Qing-Fang, Ge Hu, Qing She, Jing Yao, and Wen-Jiang Feng. Electronic structure and optical properties of Cu-doping and Zn vacancy impurities in ZnTe. *J Mol Model.* 19, no. 9: 3805-3812(2013). <https://doi.org/10.1007/s00894-013-1901-1>
39. Secuk, M. N., M. Aycibin, B. Erdinc, S. E. Gulebaglan, E. K. Dogan, and H. Akkus. Ab-initio calculations of structural, electronic, optical, dynamic and thermodynamic properties of HgTe and HgSe. *Am J. Condens. Matter Phys.* 4, no. 1: 13-19(2014). DOI: 10.5923/j.ajcmp.20140401.02
40. Ireneusz Strzalkowski, Sharad Joshi, and C. R. Crowell [1976 APPL PHYS LETT. 28 350.40] Cardona, Manuel. Infrared dielectric constant and ultraviolet optical properties of solids with diamond, zinc blende, wurtzite, and rocksalt structure. *J. Appl. Phys.* **36.7** (1965) 2181. <https://doi.org/10.1063/1.1714445>
41. E. Salman, and W. Al-zubady, Optical confinement factor of Hg_{0.2}Cd_{0.8}Te/Hg_{0.5}Cd_{0.5}Te multiple quantum well laser. College of Science for women / University of Baghdad (2018).
42. Tedjini, M. H., A. Oukebdane, M. N. Belkaid, N. Aouail, and N. Belameiri. Ab initio and Monte Carlo studies of physical properties of semiconductor radiation detectors. *Indian J. Phys.* (2021) 1-12. <https://doi.org/10.1007/s12648-020-01916-y>
43. Deligoz, Engin, Kemal Colakoglu, and Yasemin Ciftci. Elastic, electronic, and lattice dynamical properties of CdS, CdSe, and CdTe. *Physica B Condens* **373** (2006) 124-130. <https://doi.org/10.1016/j.physb.2005.11.099>
44. Woolley, J. C., and B. Ray. Solid solution in AIIBVI tellurides. *Journal of Physics and Chemistry of Solids* **13.1-2** (1960) 151-153. [https://doi.org/10.1016/0022-3697\(60\)90135-9](https://doi.org/10.1016/0022-3697(60)90135-9)
45. S. Adachi, Properties of Group-IV, III-V and II-VI Semiconductor, John Wiley and Sons Ltd, The Atrium, Southern Gate, Chichester, West Sussex PO19 8SQ, England, 2005. 978-0-470-09032-9.
46. Ireneusz Strzalkowski, Sharad Joshi, and C. R. Crowell, Dielectric constant and its temperature dependence for GaAs, CdTe, and ZnSe, *Appl. Phys. Lett.* **28** (1976) 350. doi: 10.1063/1.88755
47. T. Hattori, Y. Homma, A. Mitsuishi, and M. Tacke. Indices of refraction of ZnS, ZnSe, ZnTe, CdS, and CdTe in the far infrared. *Opt. Commun.* **7** (1973) 229-232. [https://doi.org/10.1016/0030-4018\(73\)90015-1](https://doi.org/10.1016/0030-4018(73)90015-1)
48. R. Khenata, A. Bouhemadou, M. Sahnoun, Ali H. Reshak, H. Baltache, and M. Rabah, Elastic, electronic and optical properties of ZnS, ZnSe and ZnTe under pressure. *Comput. Mater. Sci.* **38** (2006) 29. <https://doi.org/10.1016/j.commatsci.2006.01.013>
49. M. Cardona, and G. Harbeke, Absorption Spectrum of Germanium and Zinc Blende Type Materials at Energies Higher than the Fundamental Absorption Edge. *J. Appl. Phys.* **34** (1963) 813. <https://doi.org/10.1063/1.1729543>
50. Ghasemi Hasan, Mokhtari Aliand Soleimanian Vish-tasb, Introduce of ZnxHg(1-x)Te as a room temperature photodetector: ab initio calculations of the electronic structure and charge carrier transport, *Mater. Res. Express.* **5** (2018). 015910 <https://doi.org/10.1088/2053-1591/aaa740>
51. L. Ley, R. A. Pollak, F. R. McFeely, Sa P. Kowalczyk, and D. A. Shirley, Total valence-band densities of states of III-V and II-VI compounds from X-ray photoemission spectroscopy. *Phys. Rev. B* **9** (1974) 600. <https://doi.org/10.1103/PhysRevB.9.600>
52. F. Boudaiba, Ali Zaoui, and M. Ferhat. Fundamental and transport properties of ZnX, CdX and HgX (X= S, Se, Te) compounds. *Superlattice Microst* **46.6** (2009) 823. <https://doi.org/10.1016/j.spmi.2009.09.002>
53. M. Debbarma, B. Debnath, D. Ghosh, S. Chanda, R. Bhattacharjee, and S. Chattopadhyaya, First principle based calculations of the optoelectronic features of HgSxSe1-x, HgSxTe1-x and HgSexTe1-x alloys with GGA+ U functional. *J. Phys. Chem. Solids* **131** (2019) 86. <https://doi.org/10.1016/j.jpcs.2019.03.009>
54. M. Linder, GFSchatz, P. Link, HPWagner, W.Kuhn, and W. Gebhardt, *J. Phys. Condens. Matter* **4** (1992) 4601.
55. Hansen, G. L, J. L. Schmit, and T. N. Casselman. Energy gap versus alloy composition and temperature in Hg_{1-x}Cd_xTe. *J. Appl. Phys.* **53** (1982) 7099. <https://doi.org/10.1063/1.330018>
56. Miloua, R., Z. Kebab, F. Miloua, and N. Benramdane. Ab initio investigation of phase separation in Ca_{1-x}Zn_{-x}O alloys. *Phys. Lett. A* **372** (2008) 1910. <https://doi.org/10.1016/j.physleta.2007.10.077>
57. O. Madelung, W. Von der Osten, and U. Rössler, Intrinsic Properties of Group IV Elements and III-V, II-VI and I-VII Compounds/Intrinsische Eigenschaften Von Elementen Der IV. Gruppe und Von III-V, II-VI-und I-VII-Verbindungen. Vol. **22**. Springer Science & Business Media, 1986.
58. M. B. Reine, Fundamental properties of mercury cadmium telluride. *Encyclopedia of Modern Optics*, Academic Press, London 322 (2004).
59. K. H. Hellwege, and O. Madelung, *Semiconductors Physics of Group IV Elements and III-V Compounds*. Landolt-Börnstein New Series, Group III 17 (1982).
60. Okuyama, Hiroyuki, Yuko Kishita, and Akira Ishibashi. Quaternary alloy Zn_{1-x}Mg_xS_ySe_{1-y}. *textit{Phys. Rev. B}* **57** (1998) 2257. <https://doi.org/10.1103/PhysRevB.57.2257>